Chemical Physics Reviews

REVIEW ARTICLE | AUGUST 25 2025

The transformative role of machine learning in advancing MOF membranes for gas separations

Pelin Sezgin ; Seda Keskin

Check for updates

Chem. Phys. Rev. 6, 031303 (2025)
https://doi.org/10.1063/5.0278371

View Online
Export Citation

14 October 2025 06:23:21

AIP Publishing
Special Topics Open for Submissions
Learn More

AIP Publishing

Chemical Physics Reviews REVIEW pubs.aip.org/aip/cpr

The transformative role of machine learning in advancing MOF membranes for gas separations

Cite as: Chem. Phys. Rev. 6, 031303 (2025); doi: 10.1063/5.0278371
Submitted: 29 April 2025 · Accepted: 7 August 2025 ·
Published Online: 25 August 2025

View Online Export Citation CrossMark

Pelin Sezgin and Seda Keskin[a)]

AFFILIATIONS

Department of Chemical and Biological Engineering, Koç University, Rumelifeneri Yolu, Sariyer, 34450 Istanbul, Turkey

[a)]Author to whom correspondence should be addressed: skeskin@ku.edu.tr. Tel.: +90 (212) 338-1362

ABSTRACT

Metal-organic frameworks (MOFs) have been widely recognized for their potential as gas separation membranes thanks to their unique structural properties and high performance to selectively separate different types of gas molecules. MOF membranes offer great potential to replace conventional membrane materials in addressing environmental challenges like carbon capture. Experimental fabrication and testing of a single MOF membrane, even for a single type of gas separation, requires significant resources and time. Therefore, computational modeling of MOF membranes, more specifically high-throughput molecular simulations of MOFs, for various types of gas separations has been very useful in accelerating the discovery of novel MOF membranes. With the ever-increasing number of synthesized and hypothetical MOFs, reaching up to several million material candidates, brute-force molecular simulations are no longer sufficient to comprehensively explore the vast MOF space. Integration of machine learning (ML) approaches with molecular simulations has very recently accelerated materials discovery in the field of MOF membranes. ML has been very useful not only for predicting the key membrane properties of MOF membranes such as gas permeability and selectivity but also for uncovering the hidden structure-performance correlations. Compared to experimental methods and classical molecular simulations, ML offers similar accuracy at a fraction of the cost for the design and discovery of high-performing MOF membranes. This perspective focuses on the state-of-the-art ML applications in the field of MOF membranes, discusses the recent advances in this emerging field, and addresses current challenges and future directions.

© 2025 Author(s). All article content, except where otherwise noted, is licensed under a Creative Commons Attribution-NonCommercial 4.0 International (CC BY-NC) license (https://creativecommons.org/licenses/by-nc/4.0/). https://doi.org/10.1063/5.0278371

TABLE OF CONTENTS

I. BACKGROUND 1
II. MODELING OF MOF MEMBRANES. 2
A. High-throughput computational screening 2
B. Computations for MOF/polymer MMMs 4
C. Machine learning. 5
III. MOF MEMBRANES 5
IV. MOF/POLYMER MIXED MATRIX MEMBRANES . . . 8
V. OUTLOOK: OPPORTUNITIES AND CHALLENGES . . 13
A. Data 13
B. Materials 13
C. Features 13
D. Applications 13
E. AI-guided design 14

I. BACKGROUND

Metal-organic frameworks (MOFs) are crystalline porous materials made from metal ions and organic ligands.[1] They have been widely studied for various types of chemical and biological applications in the last two decades, thanks to their unique structural and chemical properties such as very large surface areas, high porosities, a large variety of pore sizes and shapes, and chemical functionalities.[2–7] The ability of tuning the pore properties of MOFs during or after their synthesis has led to the design and development of MOF materials specifically for gas separation applications. MOFs have been used either as adsorbents or membranes for separating gas molecules. Since membrane-based gas separation technology has several advantages such as lower energy consumption, reduced carbon footprint, compact and flexible design, ease of operation, and cost effectiveness compared to traditional separation methods, MOF membranes have been fabricated and examined for a large variety of gas separations.[8] These MOF membranes function by allowing the specific gas molecules to pass through their pores while blocking others, based on size, shape, or chemical affinity, thus enabling efficient separation of gases making them useful for applications like carbon capture and hydrogen purification.

Many types of MOF membranes offer higher gas selectivity or permeability than the traditional membrane materials, highlighting the

14 October 2025 06:23:21

© Author(s) 2025

great potential of MOFs to replace the conventional membrane materials. For example, several thin-film MOF membranes have been reported to achieve higher permeability and/or higher selectivity for various types of gas separations than zeolite and polymer membranes.[9,10] Despite these advantages, fabricating MOF membranes still has several challenges: Making thin, defect-free MOF membranes that retain their crystalline structure without cracks is difficult, requiring precise control over crystal growth and membrane thickness. MOFs are well-known for their high porosities, but during the membrane fabrication, ensuring uniform distribution of the pores is not straightforward. Any defects, intracrystalline gaps formed during the membrane synthesis, or misalignments in the porous structure can severely compromise the selective gas permeation properties of the MOF membrane. The lab-scale synthesis of MOF membranes has been reported to be successful to date, but scaling up the process for industrial production is always challenging since maintaining uniformity across large surfaces and ensuring reproducibility of membrane quality is difficult. The stability of MOF membranes is another concern, as they may degrade or lose their separation performance under certain conditions, such as humidity or high temperatures.

To overcome these challenges, MOFs have been also used as filler materials in polymer membranes to fabricate mixed matrix membranes (MMMs). MMMs combine the advantages of MOFs and polymers, the high gas separation performance of MOFs and the well-known technology of fabricating membranes from polymers. MOF/polymer MMMs exhibit higher gas permeability and/or selectivity than the corresponding polymer membranes and exceed the upper bound established for polymer membranes.[11,12] The critical issue in making MOF/polymer MMMs is the appropriate selection of the individual materials to ensure the compatibility and high gas separation performance. Considering the very widely varying properties of MOFs, selecting a MOF filler that will be fully compatible with a target polymer, in addition to enhancing the polymer's gas separation properties, is an important challenge. Furthermore, it has been shown that some MOF fillers can enhance both gas permeability and selectivity of a given polymer, whereas some others can only improve the gas permeability at the expense of decreasing the membrane's selectivity.[13] Therefore, finding the appropriate MOF-polymer combination is critical and not easy.

Although the very large number and diversity of MOF materials seem to be a great advantage to advance the MOF-based membrane technologies, selecting a MOF material to make a thin-film membrane or to use it as a filler in a MMM for a target gas separation is not straightforward, and currently, the field is mostly based on experimental approaches using trial-and-error. At that point, computational methods, specifically molecular simulations, play an important role in shifting the experimental efforts from a trial-and-error approach to a more efficient, data-driven strategy for material selection.[14] High-throughput computational screening (HTCS) approach, which uses classical molecular simulations to assess gas adsorption and diffusion properties of a large number of MOFs in a time-efficient manner, has been developed and used to evaluate the gas permeability and selectivity of MOF membranes and MOF/polymer MMMs.[15] These HTCS studies significantly accelerated the MOF membrane research by identifying the most useful membrane candidates among thousands of MOFs and directing the experimental efforts to these high-performing MOFs by saving significant time and resources. HTCS studies also provide an atomic-level understanding of the membrane materials that can be useful for the design of new MOFs with better gas separation performances. However, with the continuous increase in the number of synthesized MOFs and with the generation of millions of hypothetical MOFs (MOFs that are computationally generated but not synthesized yet), performing HTCS for all MOFs and analyzing this large data have become practically impossible and bring the necessity to use data science.

Machine learning (ML) integrated into the molecular simulations has very recently started to play an important role in advancing MOF membrane research for (i) efficiently exploring the vast material spaces, (ii) identifying the high-performance MOF membranes for various different types of gas separations, (iii) accelerating the discovery of new MOF membranes by predicting their gas permeation properties based on their structural data, and (iv) revealing the key features influencing membrane selectivity to guide the design of novel MOF membranes. Motivated from the recent and rapid increase in the number of ML studies focusing on design and discovery of MOF membranes and MOF/polymer MMMs, in this perspective, we addressed the role of ML in the field by reviewing the pioneering works and discussing the current opportunities and challenges of using ML in combination with molecular simulations and experiments.

II. MODELING OF MOF MEMBRANES

A. High-throughput computational screening

A detailed discussion on the current state-of-the-art in computational modeling of MOF membranes is available in the literature.[16] In this perspective, we mainly focused on performing HTCS studies involving molecular simulations and using the resulting simulation data to compute the gas permeabilities of MOF membranes. Figure 1 represents the main steps of using molecular simulations, mainly grand canonical Monte Carlo (GCMC) and molecular dynamics (MD) simulations, to compute the permeabilities of gases through a MOF structure. We note that in all HTCS studies where thousands of MOFs have been simulated, gas adsorption and diffusion properties are computed for a single MOF crystal, not for a MOF membrane configuration. Therefore, the membrane nature of MOFs such as surface functionalization or structural defects that might impact gas permeability is not directly considered in HTCS studies.

The first step of HTCS studies is to have a detailed representation of the MOF structure. The crystallographic information file (CIF) of MOFs which has all the structural information such as cell lengths, cell angles, and symmetry group has been deposited into the Cambridge Structural Database (CSD).[17] In addition to the CSD MOF database, there are several "computation-ready experimental MOF databases" which provide the CIFs of MOFs in a format that is directly usable in molecular simulations. For example, the CoRE MOF (computation-ready experimental metal-organic framework) database was first presented in 2014 and then updated in 2019 and 2024 by the addition of new MOFs and correction of some others.[18–20]

In this perspective, we mainly focused on MOFs, but it is important to mention covalent organic frameworks (COFs) for which CIFs are available in computation-ready experimental COF database (CoRE COF),[21] and in "clean uniform and refined with automatic tracking from experimental database" (CURATED COF).[22] COFs are constructed from light organic elements like carbon, hydrogen, boron, nitrogen, and oxygen, and their structures are held together by strong

14 October 2025 06:23:21

© Author(s) 2025

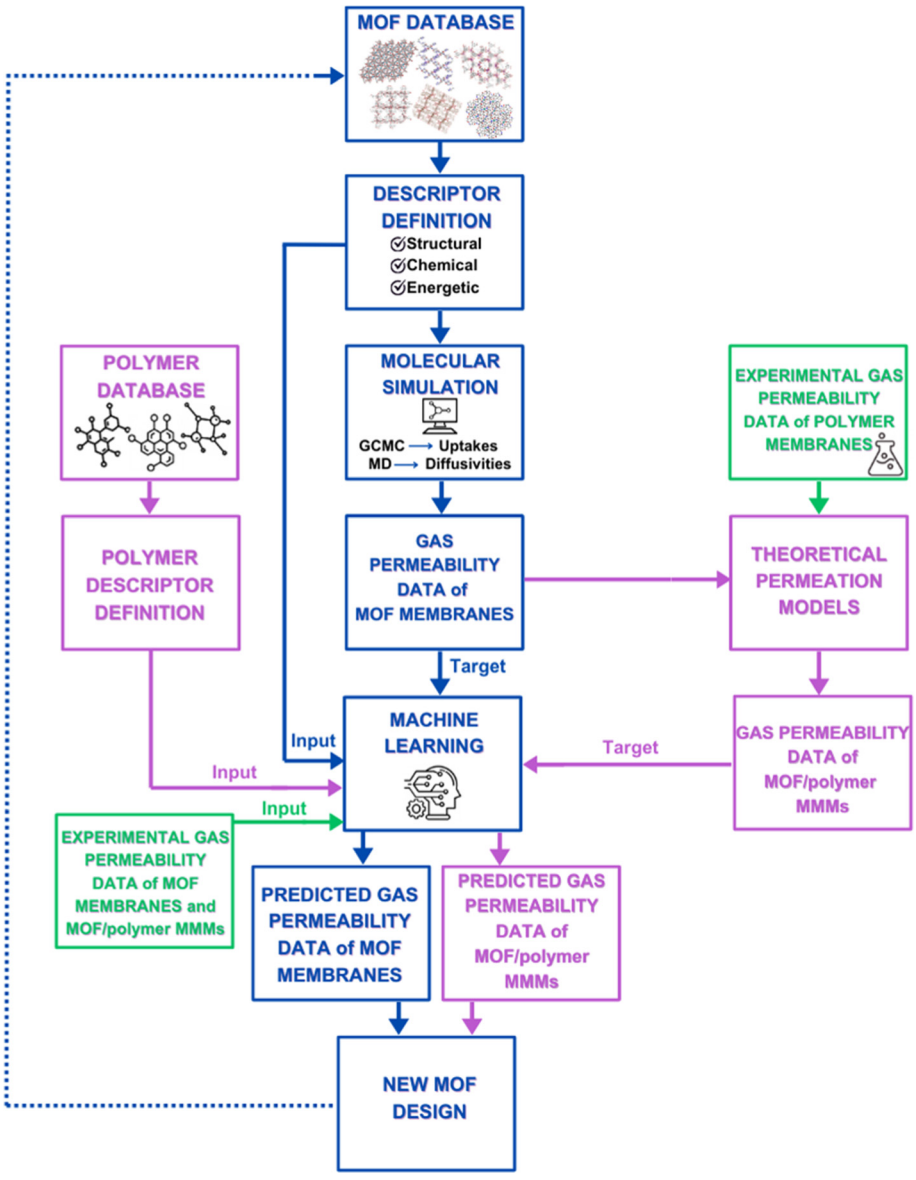


FIG. 1. Schematic of the computational methodology combining HTCS and ML for predicting gas permeation through MOF membranes and MOF/polymer MMMs.

covalent bonds in contrast to MOFs that consist of metal ions or clusters coordinated to organic ligands through coordination bonds. Since COFs typically offer greater thermal and chemical stability thanks to their purely covalent networks, they have been also examined as membrane materials both in the form of thin-film COF membranes and COF/polymer MMMs.[23]

In addition to lab-scale synthesis of MOFs and COFs, there are also numerous hypothetical MOF and COF materials that are computationally generated using either the bottom-up approach, where the building blocks extracted from synthesized materials are linked as tinker toys, or the top-down approach, where the building blocks are combined within a previously selected topology.[24–26] By using these methods, structures having more than one type of linkers can be constructed.[27] Some examples are Wilmer's hypothetical MOF (hMOF),[28] Smit's hMOF,[29] Boyd and Woo's hMOF,[30] Anion-Pillared MOFs (AP-MOFs),[31] and topologically based crystal constructor (ToBaCCo)[26] databases. Genomic COF[32] and ready-to-use database of covalent organic framework (REDD-COFFEE)[33] databases are some examples of hypothetical COF databases. These hypothetical databases provide the CIFs of computer-generated structures in a format ready for molecular simulations like CoRE databases. It is important to note that the number of structures available in hypothetical MOF and COF databases is significantly larger than the synthesized MOFs and COFs. Several of these databases also report computed structural properties of materials such as pore limiting diameter (PLD), the largest cavity diameter (LCD), accessible surface area (ASA), accessible volume (AV), and chemical information such as metal type and presence of open metal sites (OMS) of MOFs and COFs.

14 October 2025 06:23:21

© Author(s) 2025

Once the structures are obtained from these databases, classical molecular simulations can be performed. Combining GCMC and MD simulations allows for a comprehensive understanding of both the equilibrium adsorption properties and the dynamic permeation behavior of gases through the MOF structure that will be used as a membrane. For performing these simulations, software like RASPA[34] or LAMMPS[35] can be used. RASPA is developed for simulating adsorption and diffusion of molecules in nanoporous materials, and it has been very widely used to study MOFs and COFs. LAMMPS is a simulation tool for particle-based material modeling at length ranges spanning from atomic to mesoscale to continuum, a wider range compared to RASPA. It has been widely utilized to calculate the diffusion coefficients of gases in porous materials.[36–38]

GCMC simulations can be used to study the gas adsorption inside the MOF pores.[39] These simulations work by simulating the insertion and removal of gas molecules under controlled temperature, pressure, and chemical potential thus, these parameters must be set properly in addition to choosing the appropriate potential models that well describe the gas molecules and MOF structures. For example, three-site[40,41] (single-site)[42–45] models have been widely used for CO_2 and N_2 (CH_4, H_2, noble gases) molecules and generic force fields such as Universal Force Field (UFF)[46] and DREIDING[47] have been widely used for defining the MOF and COF atoms.[48] The good agreement between the experimentally reported adsorption isotherms and the results of GCMC simulations using these generic force fields has demonstrated their accuracies in many different studies.[49] There are also several studies that aimed to develop new force fields specific to MOFs to better represent the gas-MOF intermolecular interactions and intramolecular interactions within the MOF structures in GCMC simulations.[50–57]

The output of GCMC simulations are the adsorbed gas amounts computed at a given temperature and pressure (and for a composition if the simulated gas system is a mixture) and they are used as the input of MD simulations to explore the dynamic behavior of adsorbed gas molecules within the MOF structure. MD simulations allow us to observe the movement of gas molecules inside the pores over time to study molecular transport mechanisms. The output of MD simulations is the mean square displacement (MSD) of gas molecules, and these data are converted to self-diffusivity of molecule i ($D_{self,i}$) through the Einstein's relation[58] as follows:

$$D_{self,i} = \lim_{t\to\infty} \left(\mathrm{MSD}(t)/2dt\right), \tag{1}$$

$$\mathrm{MSD}\quad(t) = \left\langle \frac{1}{N} \sum_{i=1}^{N} \left(r_i(t) - r_i(0)\right)^2 \right\rangle, \tag{2}$$

where d represents the dimensionality number for diffusion at time t, N is the number of molecules, and r_i is the 3D position vector of species i.

MD simulations require more time and resources than the GCMC simulations because the former should run for sufficiently long timescales to capture the relevant transport phenomena over several different trajectories to get an accurate diffusivity coefficient. Like GCMC simulations, accuracy in force fields is critical, as the interaction between gas molecules and the MOF structure significantly influences the results. The data obtained from GCMC and MD simulations, the adsorbed gas amount (c_i) and the diffusion coefficients ($D_{self,i}$), respectively, are then used to compute gas permeability (P_i) as follows where f_i represent the partial pressure of gas molecule at the feed side of membrane. The selectivity of the MOF membrane, S_{mem}, is then calculated by using the ratio of permeabilities of two gas species

$$P_i = c_i \times D_{self,i}/f_i, \tag{3}$$

$$S_{mem} = \frac{P_i}{P_j}. \tag{4}$$

If the single-component gas permeabilities are used, ideal selectivity is obtained, whereas when the gas mixture permeabilities are used, mixture selectivity of the membrane is obtained. Current membrane literature is dominated by polymers for which the single-component gas permeabilities have been already reported.[59] Therefore, generally ideal selectivities of MOF membranes are calculated using the simulations to be compared with those of polymers.

The conditions of molecular simulations (temperature, pressure, and chemical potential) should mirror the experimental setup to ensure that the computational results are meaningful and comparable to real conditions. However, when it comes to studying a very large number of MOFs in a time and cost-efficient way, molecular simulations can be performed under "infinite dilution," which represents a hypothetical condition where the gas–gas intermolecular interactions are neglected to save computational time. Through Monte Carlo simulations, the Widom particle insertion method[60] is generally used to calculate the Henry's constants (K_0) of gases that represent gas affinities of frameworks at low pressure. Similarly, MD simulations are performed to compute self-diffusivities at infinite dilution (D_0) by switching off the intermolecular gas interactions.

By multiplying K_0 and D_0 of gas molecules, infinite dilution permeability (P_0) and selectivity (S_0) of MOF membranes can be estimated as follows:

$$P_0 = K_0 \times D_0, \tag{5}$$

$$S_0 = \frac{K_{0,i}}{K_{0,j}} \times \frac{D_{0,i}}{D_{0,j}}. \tag{6}$$

Permeability and selectivity [also referred to as permselectivity (S_{perm})] are the two main performance metrics used to assess membranes. The trade-off between selectivity and permeability is a well-known fundamental challenge in membrane science.[61,62] High gas permeability is usually observed for membranes having larger pores, which allow molecules to pass through quickly. Thus, these membranes lead to lower selectivity. On the other hand, high selectivity, often requires smaller pores that can distinguish subtle differences in molecular size or chemistry, but these structures typically result in lower gas permeability. To identify the membranes that offer both high gas permeability and high selectivity, new metrics such as membrane performance score (MPS), trade-off multiple selectivity and permeability (TMSP or TSP) are proposed as follows:

$$\mathrm{MPS} = S_{mem,i/j} \times P_i, \tag{7}$$

$$\mathrm{TMSP} = P_i \times \ln\left(S_{perm,i/j}\right) \quad \text{or} \quad \mathrm{TSP} = \ln(P_i) \times S_{perm,i/j}. \tag{8}$$

B. Computations for MOF/polymer MMMs

The permeability of gas species through the MOF (dispersed phase, also known as the filler phase) and the permeability of gas species through the polymer (continuous phase) should be known to predict the gas permeation through a MOF/polymer MMM. The

14 October 2025 06:23:21

© Author(s) 2025

literature contains a large number of theoretical permeation models that use gas permeability data from the dispersed and continuous phases to estimate the gas permeation through an MMM.[63] Among many, Maxwell[64] and Bruggeman[65] permeation models are widely used to predict MMMs' gas permeabilities in addition to some more complicated models such as Lewis–Nielsen,[66] Pal,[67] Felske,[68] and modified Felske.[63] Since the Maxwell model assumes that the streamlines related to diffusive mass transfer around filler particles are not influenced by the presence of adjacent particles, it is designed to be relevant for low filler loadings.[69] Maxwell model has been shown to be accurate for many types of MOF/polymer MMMs and is widely used thanks to its simplicity.[70] In the Maxwell model, single-component gas permeabilities through an MMM can be estimated by the following model where P_i^{MMM} represents the gas permeability of MOF/polymer MMM, P_i^P refers to the gas permeability of polymer, which can be generally obtained from the literature since a large amount of experimental data exists for polymers, P_i^{MOF} is the gas permeability of MOF which can be calculated using molecular simulations as we described above, and φ is the volume fraction of MOF fillers in the polymer

$$P_i^{MMM} = P_i^P \times \left[\frac{2\times(1-\varphi)+(1+2\varphi)\times\left(\frac{P_i^{MOF}}{P_i^P}\right)}{(2+\varphi)+(1-\varphi)\times\left(\frac{P_i^{MOF}}{P_i^P}\right)} \right]. \quad (9)$$

Using the ratio of permeabilities of two gas species, ideal selectivities of MMM can be calculated as follows:

$$S_{i/j}^{MMM} = \frac{P_i^{MMM}}{P_j^{MMM}}. \quad (10)$$

C. Machine learning

ML is a field of artificial intelligence that enables computers to learn from data. By analyzing large amounts of data, ML algorithms can identify patterns and make predictions. There are several types of ML approaches such as supervised learning where models are trained on labeled data, unsupervised learning which involves finding patterns in unlabeled data; and reinforcement learning where systems learn through trial and error by receiving feedback in the form of rewards or penalties. Technical details of the widely used ML approaches covering the supervised and unsupervised algorithms are already available in the literature.[71,72] In this perspective, we focused on how to combine the results of molecular simulations of MOFs with ML to make predictions about the gas separation performance of MOF membranes.

In ML studies, the input data are generally MOFs' structural and chemical properties, whereas the target data are the results of GCMC and MD simulations such as gas adsorption, diffusion, or permeability. As we reviewed in detail below, early ML studies used the GCMC and MD results as the target data and computed the gas permeability while the recent studies trained the ML models to directly predict the gas permeabilities and selectivities of membranes. Identifying and using meaningful descriptors are critical for developing accurate ML models.[73] Pearson correlation heat maps can be useful for assessing the correlation between input features and target property, which will be predicted by ML, and to avoid overfitting. Structural features of MOFs such as pore limiting diameter (PLD), the largest cavity diameter (LCD), porosity (ϕ), surface area (SA), geometric pore volume (PV), density (ρ), and pore size distribution (PSD) are widely used as input of ML models and these features can be directly computed using Zeo++ software.[74] Chemical features of MOFs such as atomic percentages, total degree of unsaturation (TDU), degree of unsaturation (DU), metallic percentage, and oxygen-to-metal ratio are also used as chemical descriptors in ML models, and they can be extracted from the CIFs existing in the corresponding MOF databases. Recent studies also proposed to use energetic features of MOFs as descriptors in ML models such as isosteric heat of adsorption (Q_{st}), the Henry's constants ($K_{H,i}$) of gas molecules, and energy histogram features. Widom particle insertion simulations[60] can be used for computing Q_{st} and $K_{H,i}$ of gas molecules. In addition to these computed features, experimental data available in the literature can be also used as input of ML models. For example, Brunauer-Emmett-Teller (BET) surface area of MOFs, the loading of MOF fillers used in MMMs, aperture size of MOFs, the membrane thickness, and filler size can be collected from the experimentally reported MOF/polymer MMM studies.

Once the feature and target datasets are ready, ML models can be developed. One widely used tool is tree-based pipeline optimization tool (TPOT)[75] in auto-machine learning[76] that determines the best algorithms and optimizes the hyperparameters. TPOT comprises feature engineering, model development, and evaluation of model. It is based on the evolutionary algorithm optimization. TPOT uses randomized principal component analysis (PCA),[77] a type of random principal singular value decomposition, to extract features. The scikit-learn toolkit's[77] regression algorithms can be employed for the TPOT model selection. A large variety of ML algortihms exist, and among them, Random Forest (RF),[78] Decision Tree (DT),[79] Kernel Ridge Regression (KRR),[80] Support Vector Regression (SVR),[81,82] Multilinear Regression (MLR), Gradient Boosted Trees Regression (GBTR),[83] and artifical neural networks (ANN)[84] are the mostly used ones for predicting membrane properties in the literature.

After developing ML models, ML-predicted properties are compared with the simulation or experimental results. There are various statistical accuracy metrics, such as the coefficient of determination (R^2), root mean square error (RMSE), and mean absolute error (MAE), that can be reported to assess the accuracy of models. Once the model offering the highest prediction accuracy is identified, the impact of features on the model predictions can be analyzed using the SHapley Additive exPlanations (SHAP)[85] so that one can find out the most important features determining the gas separation performances of MOF membranes. The final ML models can then be transferred to an unseen database composed of MOF structures which have not been used in the training of ML models. The idea here is to utilize the unseen data to evaluate how well an ML model can generalize to new membranes. Generally, a representative set from the unseen database can be constructed, and molecular simulations can be performed to compare the ML-predicted and simulated results for a number of MOF membranes. It is important to construct this unseen dataset to represent all properties of the entire unseen dataset so that the transferability and generalizability of the ML models can be thoroughly tested.

III. MOF MEMBRANES

Table I summarizes the current state-of-the-art in using ML for the MOF membrane field, where the number and type of MOFs studied, the type of gas separation of interest, the MOF features used as the

14 October 2025 06:23:21

© Author(s) 2025

14 October 2025 06:23:21

TABLE I. Summary of studies using ML for predicting membrane properties of MOFs.

Number of MOFs	Gas separation	Features	Predicted properties	Algorithms	Ref.
5249 synthesized MOFs	He/H_2, He/N_2, He/CH_4, H_2/N_2, H_2/CH_4, N_2/CH_4	Pore size, density, pore volume, porosity, surface area, element percentages, heat of adsorption of gases, total degree of unsaturation	Gas uptakes, diffusivities	LassoLarsCV, ETR, GBR, RF	86
7877 synthesized MOFs	He/H_2 (50/50)	Density, pore size, accessible and free volume, void fraction, partial charges of atoms, elemental content, diverse linker types	P_{He}, S_{He/H_2}	RF	87
6013 synthesized MOFs	H_2/CH_4, H_2/N_2, H_2/H_2S, H_2/O_2, H_2/CO_2, H_2/He	Pore size, surface area, porosity, density, and PSD%	P_{H_2}, TMSP	BPNN, RF, SVM, GPR, BAT, BOT, RL, SL	88
6013 synthesized MOFs	Kr/Xe (20/80)	Pore size, void fraction, surface area, density, $K_{H,i}$, $Q_{st,i}$	P_{Kr}, $S_{perm(Kr/Xe)}$, MPS	RF, DT, SVM, KNN	89
5632 synthesized MOFs	O_2/N_2	Pore size, unit cell volume, surface area, void fraction, accessible volume, atomic percentage, unsaturation degree uptakes, self-diffusivities, Henry's constants	S_{O_2/N_2}	AdaBoost, GBR, RF, SVM	90
6013 synthesized MOFs	$CH_4/(O_2+N_2)$, $H_2/(O_2+N_2)$ (N_2/O_2:78/21)	K_H, Q_{st}, pore size, density, surface area	D_i, P_i, S_{perm}	RF, DT	91
6013 synthesized MOFs	CO_2/O_2, CO_2/N_2	Volumetric surface area, void fraction, pore size, density, and PSD%	P_{CO_2}, P_{N_2}, P_{O_2}	SVM, KNN, DT, RF, GBDT, LGBM, and XGB	92
5249 synthesized MOFs	H_2/CH_4, He/CH_4, N_2/CH_4, O_2/N_2	PLD, LCD, density, molecular features	Self-diffusivities under flexibility conditions	KNN, RF, NB, GBR, KRR	93
12 723 synthesized MOFs	D_2/H_2	Pore size, void fraction, metal composition	S_{perm}	SVM, RF, GBT, DNN	94

AdaBoost: adaptive boosting, ETR: extra trees regressor, BPNN: backpropagation neural network, SVM: support vector machine, RF: random forest, GPR: Gaussian process regressor, BAT: bagged tree, BOT: boosted tree, SL: stepwise linear regression, RL: robust linear regression, XGB: extreme gradient boosting, ET: extremely randomized trees, KNN: K-Nearest Neighbor, GBDT: gradient boosting decision trees, LGBM: light gradient boosting machine, DT: decision tree, CatBoost: categorical boosting, NGBoost: natural gradient boosting, DNN: deep neural network, GBR: gradient boosting regression, NV: naïve Bayesian, KRR: kernel ridge regression, PSD: pore size distribution, PLD: pore limiting diameter, LCD: largest cavity diameter.

© Author(s) 2025

input data in ML models, and the ML-predicted membrane properties are listed in detail. We reviewed the details and key contributions of these studies to the field below.

Our group[86] was the first to integrate ML with HTCS to evaluate the performance of MOF membranes in six distinct separations: H_2/N_2, H_2/CH_4, He/H_2, He/N_2, He/CH_4, and N_2/CH_4. We conducted GCMC and MD simulations to compute He, H_2, N_2, and CH_4 uptakes and diffusivities across 5249 different MOFs at 298 K and 1 bar. By leveraging structural, chemical, and energetic characteristics of the MOFs, such as density, pore size, porosity, pore volume, surface area, elemental composition, and Q_{st} of gases, ML models were developed to accurately estimate gas uptakes and diffusivities. These uptake and diffusivity predictions were then used to compute selectivities and gas permeabilities of the entire MOF set. The ML-predicted permeabilities showed strong agreement with those from simulations, particularly for He and H_2, as illustrated in Figs. 2(a) and 2(b). In contrast, N_2 and CH_4 permeabilities were underestimated by ML in the high permeability regime ($>10^6$ Barrer), as shown in Figs. 2(c) and 2(d), though alignment was better at lower values. Analysis of the features' importance demonstrated that physical properties, such as porosity, played a dominant role in prediction accuracy compared to chemical features, such as elemental composition. Overall, our ML approach provided an efficient and reliable means of evaluating the separation capabilities of a broad range of MOF membranes, significantly reducing the computational cost and effort required for experimental fabrication and testing.

A similar approach was used to study 6013 MOF membranes for H_2 separation from various other gases, CH_4, N_2, H_2S, O_2, CO_2, and He.[88] In that work, the membrane performance metrics were directly predicted by ML. Henry's constants ($K_{H,i}$) and D_0 of single-component gases in MOFs were first calculated through GCMC and MD simulations, respectively, enabling the determination of two important membrane separation performance metrics: permeability and selectivity. Eight ML models were developed to predict H_2 permeability and trade-off multiple selectivity and permeability (TMSP), when the structural features of the MOFs such as VSA, ϕ, PLD, LCD, ρ, and PSD% were used as input. Two ML algorithms, GPR and RF, were selected for predicting the membrane performance metrics. The results revealed that VSA, PLD, and LCD are the most critical features for the prediction of H_2 permeability and TMSP of the top-performing MOF membranes.

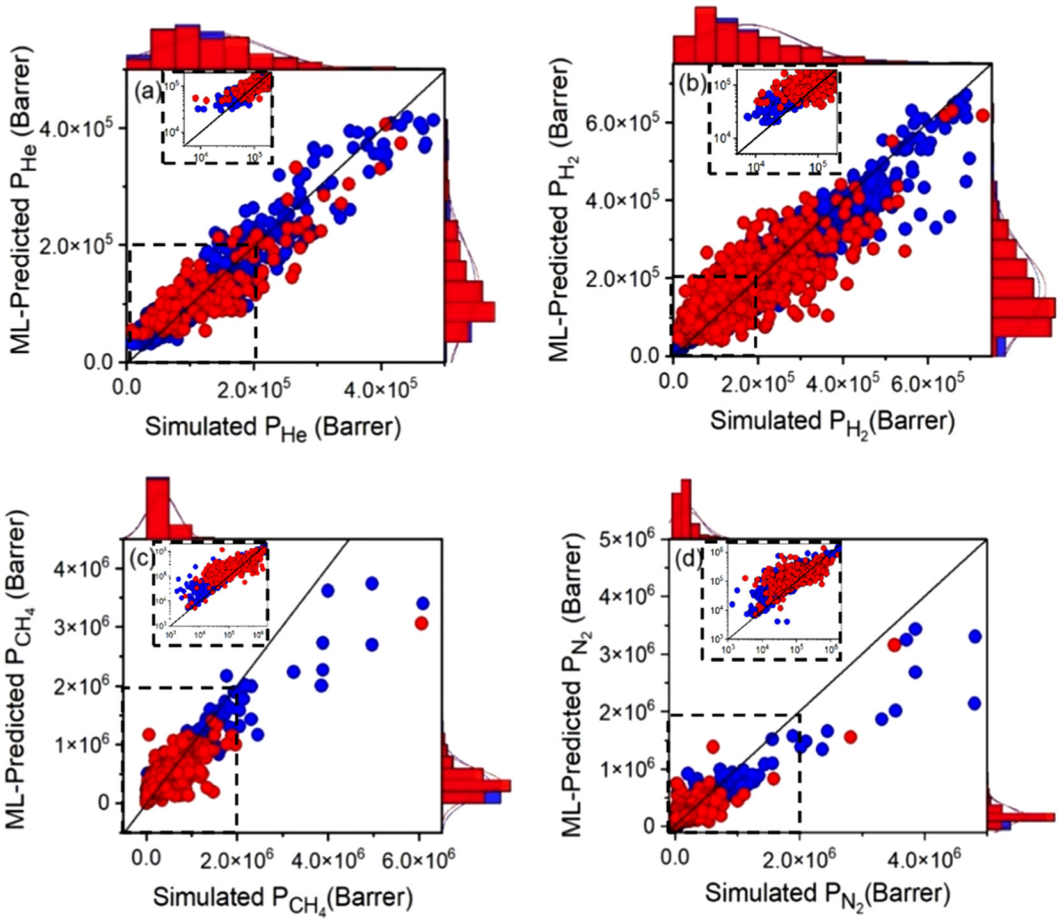


FIG. 2. ML-predicted permeabilities of (a) He, (b) H_2, (c) CH_4, and (d) N_2 in MOF membranes in comparison with simulated values. Blue symbols indicate training data, while red symbols represent test data. Adapted with permission from Daglar and Keskin, ACS Appl. Mater. Interfaces **14**(28), 32134–32148 (2022). Copyright 2022 Authors, licensed under a Creative Commons Attribution (CC BY) license.[86]

14 October 2025 06:23:21

© Author(s) 2025

The top-performing 15 MOF membranes, which were selected to have high P_{H_2}(>50 Barrer) and $S_{perm,\,H_2/N_2}$(>30) and ranked based on TMSP, were found to have high performance with P_{H_2} and TMSP values between 60.6 and 935.4 Barrer and 400.1–8560.8, respectively.

HTCS was combined with ML to study the membrane-based Kr/Xe separation using MOFs.[89] GCMC and MD simulations were performed for 6013 MOFs to compute the adsorption and diffusion data, respectively, for Xe/Kr:20/80 mixture at 1 bar, 298 K, and then these data were used to assess gas permeabilities and selectivities of the MOF membranes. Structural properties, such as void fraction, VSA, ρ, PLD, LCD, and energetic properties ($K_{H,i}$ and Q_{st}) of MOFs were used as input for ML models. A new performance index, MPS, the multiplication of the permeability (P_{Kr}) and selectivity ($S_{Kr/Xe}$), was introduced and ML model was trained to assess the MPS scores of MOF membranes. RF and XGB models were used to predict P_{Kr}, $S_{Kr/Xe}$, and MPS. XGB models exhibited better agreement between ML predictions and simulation results for the prediction of three performance indicators. Figure 3(a) shows the prediction power of XGB models with high R^2 (0.96) value whereas Fig. 3(b) demonstrates that PLD is the most important descriptor to assess MOF membranes' performance indicators P_{Kr}, $S_{perm\ (Kr/Xe)}$, and MPS, with the relative importance values of 16.9%, 26.1%, and 13.7%, respectively. The best MOF membranes were identified to have P_{Kr} >1000 Barrer and $S_{perm\ (Kr/Xe)}$ >10, and their linkers were analyzed in detail. It was shown that MOFs with aromatic rings, hydroxyl groups, oxygen atoms connected by double bonds, and Zn centers have improved Kr/Xe separation performance.

For studying ternary $CO_2/N_2/O_2$ separation, the permeabilities of pure CO_2, N_2, and O_2 were calculated in 6013 MOF membranes through a combination of GCMC and MD simulations.[92] Several performance metrics, P_{CO_2}, P_{O_2}, P_{N_2}, $S_{perm(CO_2/O_2)}$, and $S_{perm(CO_2/N_2)}$ were calculated and then predicted using different ML algorithms. Six structural descriptors, which are volumetric surface area (VSA), void fraction, PLD, LCD, density, and pore size distribution percentage, were used as input for ML. Results showed that LCD for P_{CO_2} and $S_{perm(CO_2/O_2)}$ predictions, porosity for P_{O_2} and P_{N_2} predictions, and PLD for $S_{perm(CO_2/N_2)}$ predictions are the most important features.

A recent study combined HTCS with ML to rapidly screen high-performance COF membranes for H_2S and CO_2 removal from natural gas.[95] GCMC and MD simulations were carried out to simulate the single-component H_2S, CO_2, and CH_4 adsorption and diffusion in 788 synthesized COFs at 10 bar, 298 K. These data were then used to predict the gas permeability and selectivity of COF membranes. ML models were constructed for the adsorption, diffusion, and permeability of gases in COFs, where structural (PLD, LCD, void fraction, etc.) and chemical (atomic percentages, total degree of unsaturation, total electronegativity, etc.) features were used. Analysis of the ML models highlighted that the volume fraction (VF) has a significant contribution to gas permeability, and 500 hypothetical COFs (hCOFs) were sampled based on VF to combine with 788 synthesized COFs for training ML models with better generalization capability. Figure 4 shows that ML predictions for the training set (1288 COFs) and the predicted set (unseen 14 457 hCOFs) are in good agreement. Figure 4(a) presents that H_2S permeabilities of 30 hCOFs exceeded 6×10^5 Barrer and there are many highly permeable hCOF membranes compared to synthesized COFs. Figure 4(b) shows that there are several high-performance COF membranes close to the upper bound for CO_2/CH_4 separation. The highest H_2S/CH_4 and CO_2/CH_4 selectivities were predicted as 3.6 and 1.9, respectively. These results are comparable to the selectivities of the top-synthesized COFs with high-performance membrane separation properties.

IV. MOF/POLYMER MIXED MATRIX MEMBRANES

Considering the very large number of available polymers and MOFs, it is difficult to find the best match for a MOF and a polymer to create high-performance MMMs. To select the MOF fillers of MMMs, HTCS of MOFs should be performed, which requires running GCMC and MD simulations to compute gas adsorption and diffusion properties of every MOF, and these data are combined with the polymer's gas

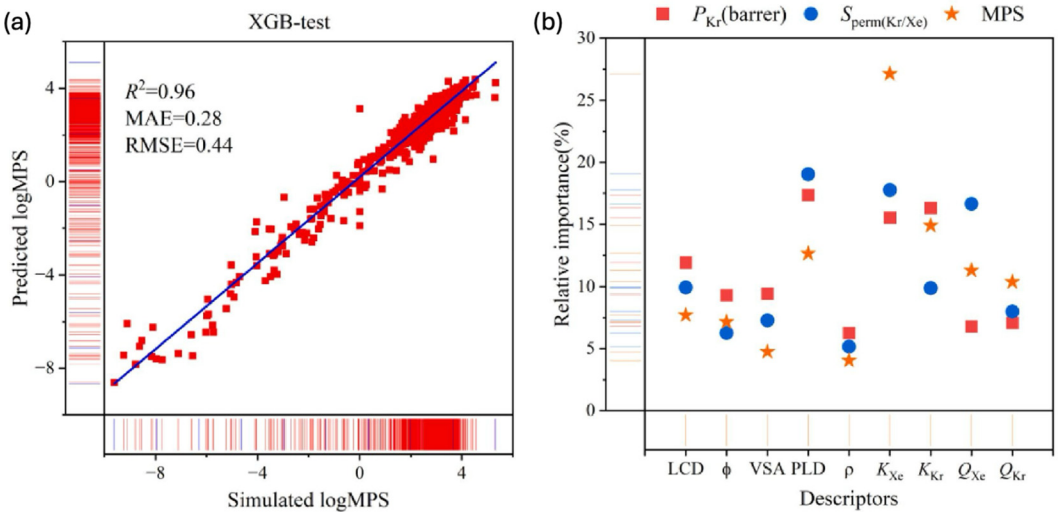


FIG. 3. Comparison of the ML-predicted and simulated results for logMPS and the relative importance values of the nine descriptors of MOF membranes obtained from the ML model. Adapted with permission from Huang *et al.*, Chem. Eng. Sci. **280**, 119031 (2023). Copyright 2023 Elsevier.

14 October 2025 06:23:21

© Author(s) 2025

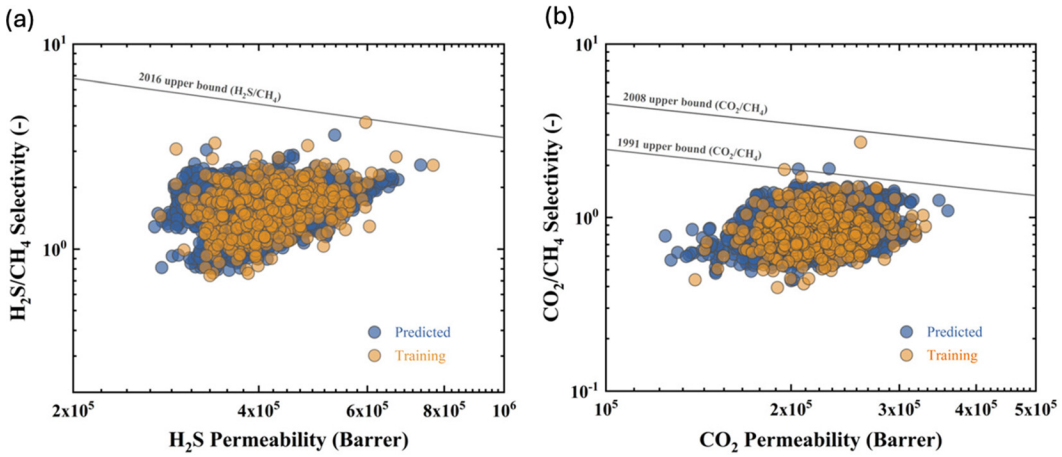


FIG. 4. ML-predicted H_2S/CH_4 and CO_2/CH_4 selectivities along with H_2S and CO_2 permeabilities of COF membranes. Adapted with permission from Xin *et al.*, Ind. Eng. Chem. Res. **63**(18), 8369–8382 (2024). Copyright 2024 American Chemical Society.[95]

permeability data through a theoretical permeation model. All these molecular simulations and theoretical permeation model calculations must be repeated for every single MOF and polymer, which is computationally very demanding. Table II summarizes the studies using ML for predicting gas separation properties of the MOF/polymer MMMs, where the number of MMMs and polymers, the type of gas separation, the MOF and polymer features used as the input data, and the ML-predicted properties are listed in detail.

Our group[86] introduced a computational framework, illustrated in Fig. 5, to efficiently and accurately evaluate the gas separation performance of a large number of MOF/polymer MMMs using ML. By combining ML with HTCS, we examined the potential of 31 494 distinct MOF/polymer MMMs for six key industrial gas separations: He/H_2, He/N_2, He/CH_4, H_2/N_2, H_2/CH_4, and N_2/CH_4. The MOF database was first filtered based on pore size and surface area to ensure gas adsorption within the MOF pores. A set of structural, chemical, and energetic descriptors, including pore size, atom types, metallic percentage, and Q_{st}, were computed to serve as input features for the ML models. GCMC and MD simulations were conducted to obtain uptake and diffusion data for He (677 MOFs), H_2 (2715 MOFs), N_2 (5224 MOFs), and CH_4 (5215 MOFs) at 298 K and 1 bar. This large MOF data were used to develop ML models. The ML-predicted gas permeabilities of MOFs were then combined with experimentally measured permeabilities of six polymers via the Maxwell model to estimate the separation performance of the 31 494 MOF/polymer MMMs. After validating the strong predictive capability of our ML models, we transferred them to evaluate 1000 hypothetical MOF/polymer MMM combinations. The predicted permeabilities showed strong consistency with both molecular simulation results and experimental data from various MOF/polymer systems, such as CuBTC/Matrimid, MgMOF-74/PIM-1, and MIL-53/Matrimid. This confirms that our ML approach offers a reliable and efficient alternative to labor-intensive experiments and computationally intensive molecular simulations.

A very large number of MMMs, 456 872 different types of MOF/polymer combinations, were studied for He/CH_4 separation, combining HTCS and ML.[96] The gas permeability data of 8787 MOF were computed at infinite dilution, 308 K, using the GCMC and MD simulations which calculated the Henry's coefficients and self-diffusivities of gases, respectively. The infinite dilution permeability data of MOFs were combined with the gas permeability data of 26 polymers collected from the literature and fed to the Maxwell model to get the gas permeability of the MMMs. Four different ML algorithms were studied, where He and CH_4 permeabilities of polymer, He/CH_4 selectivity of polymer, the volume fraction of MOFs in MMMs, temperature, and several pore properties of the MOFs were used as input to predict the gas permeability of MMMs. The results of the ML models suggested that the polymer matrix should have a He selectivity >900, He permeability >1600 Barrer, and MOF fillers should have a pore size 2.6 Å<PLD < 3.2 Å to achieve high-performance MMMs for He/CH_4 separation.

These two studies we reviewed performed GCMC and MD simulations to produce the gas permeability data of a very large number of MOFs that can be used as fillers in MMMs, since the experimental gas permeability data of MOFs is very limited in the literature. Zhang's group[97] followed a different strategy and trained their ML models using the available literature data on MOF-based MMMs, involving 36 types of MOFs and 41 different types of polymers, for CO_2/CH_4 separation. As represented in Fig. 6, they integrated ML models with the experiments by using the guidelines offered by ML for the optimal design of MOFs. ML models revealed that MOF structures with pore size >1 nm and surface area of ~800 $m^2\ g^{-1}$ can be useful fillers for MMMs. Based on this outcome, two new types of MOFs, Cu-CAT-1 and Cu-THQ, were synthesized and used as fillers in Pebax-2533 and PIM-1 polymers to fabricate MOF/polymer MMMs. These MMMs were reported to have high CO_2 separation performances: For example, blending Cu-CAT-1/PIM-1 MMM at 20 wt. % MOF loading was measured to have higher CO_2 permeability (8339 Barrer) and CO_2/CH_4 selectivity (15.6) compared to those of pristine PIM-1 (4185 Barrer and 14.6), which surpassed the 2008 upper bound. Therefore, this work is a very important example of using ML to guide the design, fabrication, and testing of high-performance MOF/polymer MMMs.

The dataset provided for CO_2/CH_4 separation performances of MOF-based MMMs by Zhang's group, including both pure and

14 October 2025 06:23:21

© Author(s) 2025

14 October 2025 06:23:21

TABLE II. Summary of studies using ML for predicting MOF/polymer MMM properties.

Number of MOF/polymer MMMs	Gas separation	Features	Predicted properties	Algorithms	Ref.
31 494 (six polymers)	He/H_2, He/N_2, He/CH_4, H_2/N_2, H_2/CH_4, N_2/CH_4	Pore size, density, pore volume, porosity, surface area, element percentages, heat of adsorption of gases, total degree of unsaturation	Gas uptakes, diffusivities	LassoLarsCV, ETR, GBR, RF	86
456 872 (26 polymers)	He/CH_4	Pore size, density, VSA, pore volume, porosity, temperature, P_{He}, P_{CH_4}, S_{He/CH_4} of polymer, volume fraction of MOFs in MMMs, polymer, and MOF type	P_{He}, S_{He/CH_4}	XGB	96
648 (41 polymers)	CO_2/CH_4, CO_2/N_2	MOF type, polymer type, pore size, BET area, P_i and $S_{i/j}$ of pure polymer, temperature, pressure, filler size, thickness	P_{CO_2}, S_{CO_2/CH_4}	RF	97
54 117 (nine polymers)	CO_2/CH_4, CO_2/N_2, CO_2/H_2, CO_2/O_2 (50/50)	Density of polymer, polymers' fractional free volume, pore sizes of MOFs, density ratio (MOF/polymer), density of MOFs, surface area of MOF, K_H, porosity, PSD%, Q_{st}	P_{CO_2}, TSP, S_{perm}	BPNN, RF, XGB, ET, KNN, GBDT	98
291 (19 polymers)	CO_2/N_2	MOFs BET surface area, pore size of MOFs, polymer type, filler loading, pressure, temperature	P_{CO_2}, S_{CO_2/N_2}	ANN, RF, SVM	99
3593 IL/MOF Composites (one IL)	CO_2/N_2 (15/85)	pore size, density, surface area, accessible and free volume, unsaturation degree, metallic percentage, number of atoms	P_{CO_2}, S_{CO_2/N_2}	RF	100
2873 IL/MOF Composites (five ILs)	He/H_2 (50/50)	Pore size, surface area, element percentages, IL content (%)	P_{He}, P_{H_2}, lnMPS	XGB, CatBoost, LGBM, GBR, NGBoost	101

© Author(s) 2025

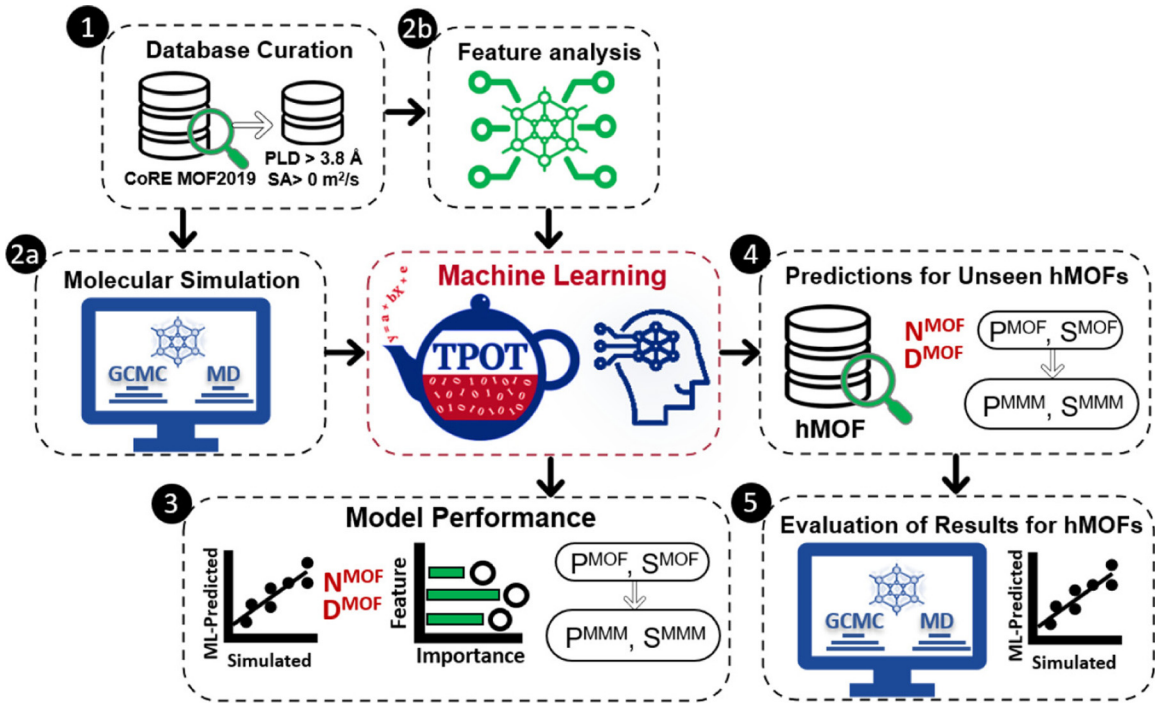


FIG. 5. Computational workflow to assess the gas separation performances of MOF/polymer MMMs combining HTCS and ML approaches. Reproduced with permission from Daglar and Keskin, ACS Appl. Mater. Interfaces **14**(28), 32134–32148 (2022); Copyright 2022 Authors, licensed under a Creative Commons Attribution (CC BY) license.[86]

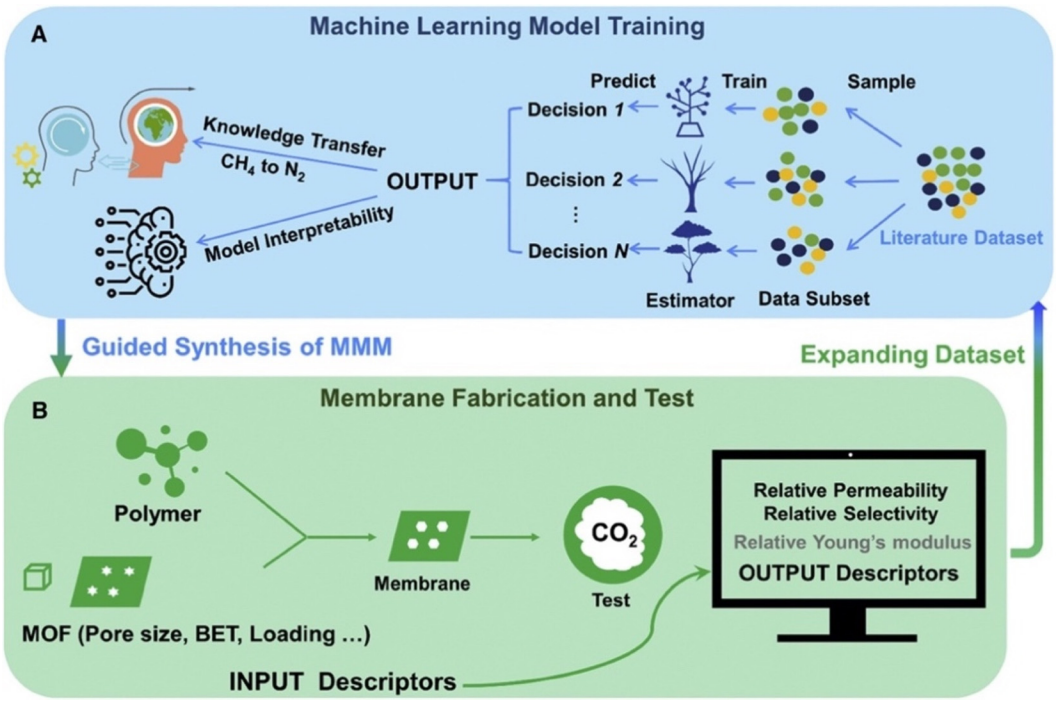


FIG. 6. Proposed workflow showing the cycle of ML-guided MOF design and MOF/polymer MMM fabrication for CO_2 capture. Adapted with permission from Guan *et al.*, Cell Rep. Phys. Sci. **3**(5), 100864 (2022). Copyright 2022 Elsevier.[97]

14 October 2025 06:23:21

© Author(s) 2025

mixed gas data, was then used to develop ML models to accurately assess gas permeability and selectivity of MMMs.[102] A novel optimized extreme learning machine was proposed where the descriptors are fingerprints for polymer featurization, physical and structural features of MOFs as well as operating conditions. Results of models revealed that the cage size of the MOF and the molecular descriptors of the polymers are the most significant parameters in estimating the permeability of MOF/polymer MMMs, while the filler loading amount and pressure were found to be critical factors determining the selectivity. The cage size of the MOF was reported to have an important role, where smaller cages lead to higher CO_2 permeability, and higher temperatures also result in increased gas permeability. Thus, the ML models developed in that work demonstrated the proper selection of the MOF filler based on the cage size, the polymer matrix, and operating temperature for developing high-performance MOF-based MMMs.

A recent work focused on predicting the CO_2 separation performances of MOF/polymer MMMs using HTCS, ML, and big data mining.[98] 54 117 different types of MMMs composed of 9 polymers and 6013 MOFs were studied for the separation of CO_2 from CH_4, N_2, H_2, and O_2 to identify the best-performing combinations of MOFs and polymers that lead to MMMs exceeding Robeson's upper limit. GCMC and MD simulations produced the gas adsorption and diffusion properties of MOFs at 10 bar, 298 K, and these data were used to compute the gas permeability and selectivity of MOFs. The trade-off between selectivity and permeability (TSP) was computed for MMMs based on the Maxwell model for CO_2/N_2, CO_2/CH_4, CO_2/H_2, and CO_2/O_2 separations. Different ML models were trained to predict the TSP of MMMs. Feature analysis is shown in Figs. 7(a) and 7(b) demonstrates that PLD, LCD, and $Q_{st(CO_2)}$ values of MOFs and the fractional free volume (FFV) and density (ρ_{poly}) of polymers are among the most important features to estimate TSP values for CO_2/N_2 and CO_2/CH_4 separations. Features of polymers are significant for both gas separations since they are fundamental to MMMs' gas permeability and selectivity. While a larger FFV may increase permeability by providing more channels and pores for gas molecules to permeate, a smaller FFV can improve selectivity by preventing larger molecules from passing through.

The top-performing MMMs were identified by ranking TSP values of CO_2/N_2, CO_2/CH_4, CO_2/H_2, and CO_2/O_2 separations and categorized into six groups. Common features of these MMMs, such as MOFs' pore size, porosity, VSA, Q_{st}, and polymers' FFV, ρ_{poly} for CO_2/N_2 and CO_2/CH_4 separations, were investigated as shown in Figs. 7(c) and 7(d). The significance of polymer features was found to be higher in the entire MMM dataset than in the top 6000 dataset for both separations, whereas MOF features, especially PLD and LCD, were more important for the top 6000 MMMs. These results highlighted the benefit of using ML for revealing the importance of polymers' and MOFs' properties in assessing the gas separation performance of MOF/polymer MMMs.

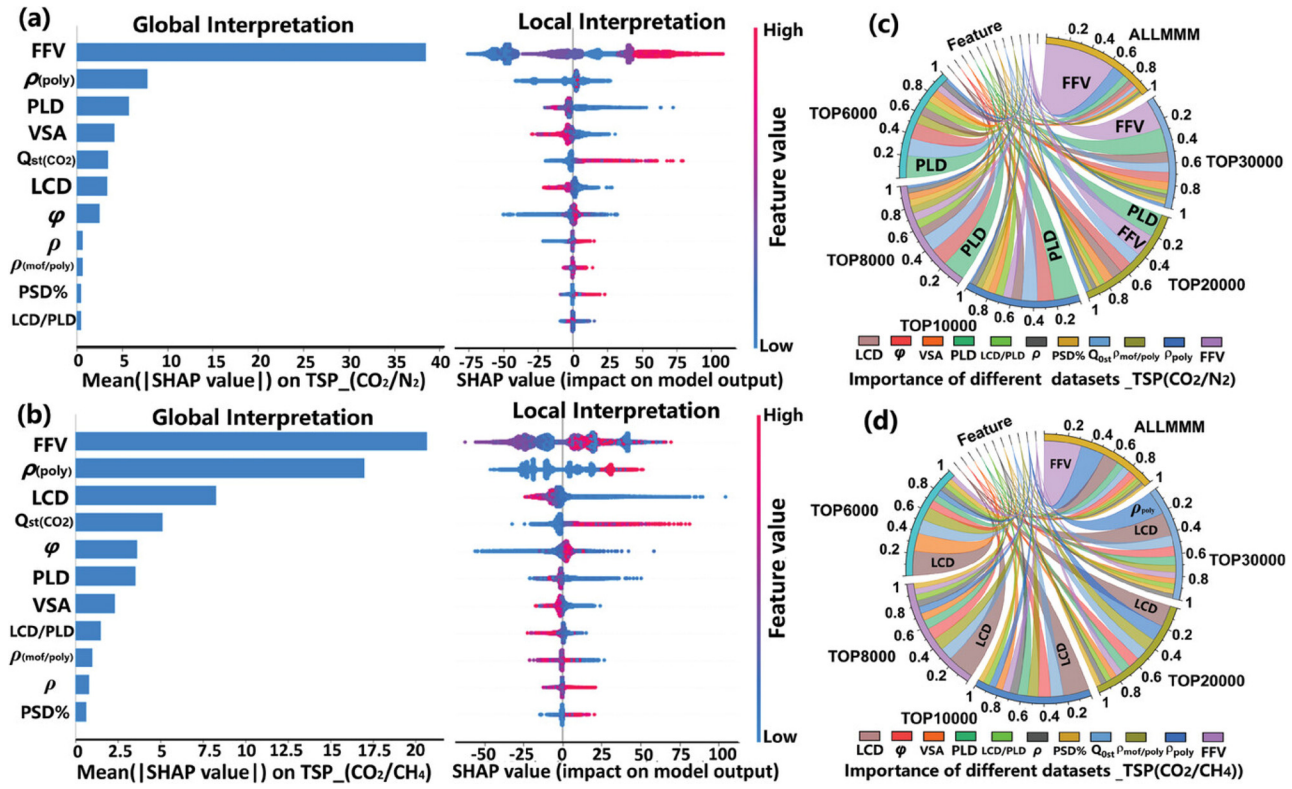


FIG. 7. Global and local interpretations for the feature importance analysis on (a) TSP (CO_2/N_2) and (b) TSP (CO_2/CH_4) predictions. Relative importance of features for (c) TSP (CO_2/N_2) and (d) TSP (CO_2/CH_4) predictions on different datasets. Reproduced with permission from Wan *et al.*, Adv. Sci. **12**(16), 2405905 (2025). Copyright 2025 Wiley.[98]

14 October 2025 06:23:21

© Author(s) 2025

In addition to pristine MOFs, MOF-based composite materials have been also studied as fillers in MMMs. Among many different MOF-based composites, ionic liquid (IL)-incorporated MOFs play an important role in gas adsorption and separation applications since incorporation of an IL molecule into the pores of MOFs, represented as IL@MOF composites in the literature, has been shown to significantly improve the gas selectivity of pristine MOFs.[103] Selecting the most appropriate IL@MOF composites for a given polymer and a target gas separation is very demanding considering the extensive time and resource requirement in molecular modeling of these composites which includes finding the optimized geometries of cation-anion pairs of an IL, the correct configuration of IL inside the MOF, and performing molecular simulations for the IL/MOF composites that have thousands of atoms. Thus, the rational selection of IL@MOF fillers using ML is important for fabricating high-performance MMMs.

To address this, Zhong's group integrated ML with molecular simulations to investigate large numbers of IL@MOF composites as membranes.[100] They constructed a database consisting of 3593 different types of IL@MOF composites by inserting an IL, [NH_2-Pmim][Tf_2N], into MOFs and performed molecular simulations to examine these composites' CO_2 permeability and CO_2/N_2 selectivity. Using various geometric (ρ, PLD, ASA, and AV) and chemical (number of atoms, degree of unsaturation, metallic percentage, oxygen-to-metal ratio, nitrogen-to-oxygen ratio) descriptors of IL@MOF composites, ML models were trained to predict CO_2/N_2 selectivity and CO_2 permeability. The accessible volume and gravimetric accessible surface area were found as the key factors in predicting the membrane selectivity and CO_2 permeability of the composites, respectively. [NH_2-Pmim][Tf_2N]@ZIF-67 composite was identified to be promising as a filler for PIM-1 polymer. The synthesis, characterization, and gas separation performance evaluation of IL@MOF-based MMMs were carried out to validate the accuracy of predictions. Experimental results show that CO_2 permeability (9536 Barrer) and CO_2/N_2 selectivity (31.1) of [NH_2-Pmim][Tf_2N]@ZIF-67/PIM-1 MMM were higher than the neat PIM-1 and ZIF-67/PIM-1 MMMs, having permeabilities of 4310 and 7190 Barrer and selectivities of 22.6 and 22.4, respectively. Thus, harnessing HTCS and ML was shown to be useful for selecting complex filler materials such as IL@MOF fillers for fabricating MMMs with excellent performance.

V. OUTLOOK: OPPORTUNITIES AND CHALLENGES

Using ML in the field of MOF membranes has the potential to significantly accelerate the design, discovery, and performance optimization of materials for various gas separation processes. Integration of ML to molecular simulations and experiments is an emerging field and is quickly growing. However, several challenges still exist and hinder the widespread adoption of ML in this field, and these challenges can be considered as future research directions.

A. Data

Like many other fields, ML models in MOF membrane research often suffer from a lack of high-quality, standardized datasets produced by experimental and computational research. While ML models require large, high-quality datasets for effective training, experimental data on key membrane properties such as permeability and selectivity are typically sparse in the literature due to the complexity of MOF membrane fabrication. There is also very limited data on how gas permeability and selectivity of the membrane change with the operating conditions like pressure and temperature. Membrane performance is affected by numerous factors other than operating conditions, such as fouling and aging properties of the MOFs, but data on these variables are often not reported. Moreover, membrane performance testing can vary significantly across experimental setups and measurement protocols, resulting in non-uniform datasets. Compared to experimental data, there is more computational data related to MOF membranes, thanks to many simulation studies that we reviewed. However, the number of molecular simulation studies on MOF membranes is still very small compared to those on MOF adsorbents since performing GCMC simulations is much practical and faster than simulating gas diffusion via computationally intensive MD simulations. Performing MD simulations to compute diffusivities for various gases in many MOFs will produce an important dataset for future ML studies of MOF membranes.

B. Materials

Current ML studies on MOF membranes often focus on synthesized MOF databases, as the goal is typically to identify MOFs with high gas separation performance that can then be fabricated into membranes with well-established experimental synthesis procedures. However, several hypothetical MOF databases offer a more diverse range of structures that may lead to even better membrane materials. There are more than millions of hypothetical MOF and COF structures that can be examined for membrane-based gas separations, and future ML studies can focus on accelerating the screening of these hypothetical material databases to broaden the scope of potential discoveries.

C. Features

Feature engineering can be difficult due to the complexity of membrane materials and their behavior under different conditions. The key features influencing performance may not always be obvious, and selecting the most important features for ML models requires a good understanding of both membrane materials and process mechanisms. ML studies that we reviewed used simple, easily measurable or computable structural features of MOFs as descriptors such as pore size, surface area, and porosity. However, MOFs have multidimensional characteristics, such as morphology, chemical composition, surface properties, and capturing these in a format usable for ML algorithms can be the focus of future studies. Since the membrane-based gas separation performance of MOFs strongly depends on the conditions, it would be very useful to describe temperature, pressure, and composition of the gas mixture as features of ML models. It is also important to develop ML models with features that can be easily defined by the users. For example, descriptors such as pore size of the MOF or temperature can be easily known/measured/calculated by a researcher, whereas more complicated descriptors such as the bits of linkers of MOFs may not be directly known/easily measurable/calculatable by every researcher.

D. Applications

Studying the transferability and generalizability of ML models is essential for the broader application of ML in membrane technology. In almost all ML studies on MOF membranes, models were trained and tested on seen material data. Future studies on the transferability of models to unseen material sets, for example, training ML models for

14 October 2025 06:23:21

© Author(s) 2025

MOF membranes and testing their transferability by applying them to unseen COF membranes or other porous membranes, is an important future direction. Furthermore, testing the transferability of ML models across different types of gas separation technologies can save enormous time and resources. ML models trained on data from one gas separation system may not perform well when applied to another gas separation system without significant retraining or adjustments. A recent study[97] highlighted the importance of developing transferable ML models to build the most effective MMMs for different CO_2 binary separation systems. Data on MOF-based MMMs for CO_2/N_2 separation were extracted from the literature, which is much smaller than that of CO_2/CH_4 and has more missing values, which limits the development of ML for CO_2/N_2 separation. Therefore, ML models predicting CO_2/CH_4 separation performance were applied to CO_2/N_2 separation. Finally, almost all the MOF membrane literature is focusing on selective separation of a gas molecule from others but one may desire the membrane to be selective to multiple types of gases, rendering the ML membrane design a multi-objective optimization problem. This is a relatively less explored area in ML for membrane design and thus an intriguing future opportunity.

In this perspective, we specifically focused on MOF membranes used for gas separations, but MOFs have also potential in liquid separation. For example, a recent work[104] showed that a water-stable MOF-based membrane (polydopamine (PDA) functionalized MOF separating layer on ceramic membrane (CM) support (PDA-s-UiO-66-NH_2-CM)] exhibited high permeability, antifouling properties, and excellent oil-water separation efficiency. The membrane developed through a solvothermal self-assembly strategy demonstrated air superhydrophilicity and underwater superoleophobicity, ensuring minimal oil adhesion. PDA-s-UiO-66-NH_2-CM has a low tendency to become clogged by oil droplets during separation, as evidenced by the membranes' exceptional stability after several continuous test cycles. ML models were employed to predict and optimize separation performance for liquid-phase separations.

E. AI-guided design

Finally, it is crucial to recognize that designing MOF membranes for specific applications requires evaluating not only their separation performance but also key factors such as ease of synthesis and stability of these membranes.[105] Future ML studies should therefore prioritize optimizing membrane synthesis conditions and predicting the long-term stability of membranes. Considering that ML approaches have recently been applied to bulk MOFs to predict their synthesis conditions and stabilities,[106] extending the similar approach to MOF-based membranes should be possible. A pioneering example of this approach was recently reported where ML was used to optimize the synthesis conditions of a surface-anchored MOF (SURMOF) structure to improve its stability and crystallinity, and then utilized to convert this high-quality MOF-thin films into a polymeric membrane, preserving the enhanced selectivities for H_2/CO_2 gas separation.[107,108]

A key development aligned with this objective is the rise of self-driving laboratories (SDLs). SDL refers to a system that integrates automated experimentation with data-driven decision-making to accelerate the application of the scientific method and advance materials discovery.[109] SDLs combine ML, automation, and robotic experimentation into closed-loop systems that autonomously design, synthesize, characterize, and evaluate materials for a wide variety of applications. SDLs focus on optimizing the function of materials in addition to optimizing the synthesis conditions for crystalline porous materials like MOFs. In these laboratories, ML models iteratively guide the selection and execution of the next optimal experiment in real time, dramatically accelerating discovery. As demonstrated in pioneering work,[107] SDLs reduce the time, cost, and effort associated with identifying and validating high-performance MOF membranes. By combining HTCS, robotic synthesis, and rapid experimental evaluation, SDLs close the gap between computer predictions and experimental results and support fully AI-guided membrane design for gas separations.

For a fully AI-guided MOF membrane design, integrating ML with experimental testing is essential, paving the way for automated laboratories. Large language models have the potential to autonomously design, plan, and even conduct experiments for synthesizing various MOF membranes. As always, interdisciplinary collaboration among experts in chemistry, chemical engineering, materials science, and data science will be vital in unlocking the full potential of this approach.

ACKNOWLEDGMENTS

S.K. acknowledges funding by the European Union (ERC, STARLET, 101124002). Views and opinions expressed are, however, those of the author(s) only and do not necessarily reflect those of the European Union or the European Research Council. Neither the European Union nor the granting authority can be held responsible for them.

AUTHOR DECLARATIONS

Conflict of Interest

The authors have no conflicts to disclose.

Author Contributions

Pelin Sezgin: Conceptualization (equal); Investigation (equal); Writing – original draft (equal); Writing – review & editing (equal). **Seda Keskin:** Conceptualization (equal); Investigation (equal); Project administration (equal); Supervision (equal); Writing – original draft (equal); Writing – review & editing (equal).

DATA AVAILABILITY

Data sharing is not applicable to this article as no new data were created or analyzed in this study.

REFERENCES

[1]S. Kitagawa, "Metal–organic frameworks (MOFs)," Chem. Soc. Rev. **43**(16), 5415–5418 (2014).
[2]O. K. Farha, I. Eryazici, N. C. Jeong, B. G. Hauser, C. E. Wilmer, A. A. Sarjeant, R. Q. Snurr, S. T. Nguyen, A. Özgür Yazaydın, and J. T. Hupp, "Metal–organic framework materials with ultrahigh surface areas: Is the sky the limit?" J. Am. Chem. Soc. **134**(36), 15016–15021 (2012).
[3]W. Xuan, C. Zhu, Y. Liu, and Y. Cui, "Mesoporous metal–organic framework materials," Chem. Soc. Rev. **41**(5), 1677–1695 (2012).
[4]H. Furukawa, K. E. Cordova, M. O'Keeffe, and O. M. Yaghi, "The chemistry and applications of metal-organic frameworks," Science **341**(6149), 1230444 (2013).
[5]M. Kim, K. K. Leong, N. Amiralian, Y. Bando, T. Ahamad, S. M. Alshehri, and Y. Yamauchi, "Nanoarchitectured MOF-derived porous carbons: Road to future carbon materials," Appl. Phys. Rev. **11**(4), 041317 (2024).

14 October 2025 06:23:21

© Author(s) 2025

[6]K. A. Forrest, G. Verma, Y. Ye, J. Ren, S. Ma, T. Pham, and B. Space, "Methane storage in flexible and dynamical metal–organic frameworks," Chem. Phys. Rev. **3**(2), 021308 (2022).
[7]H. A. Bicalho, V. Quezada-Novoa, and A. J. Howarth, "Metal–organic frameworks for the generation of reactive oxygen species," Chem. Phys. Rev. **2**(4), 041301 (2021).
[8]Y. Yampolskii, "Polymeric gas separation membranes," Macromolecules **45**(8), 3298–3311 (2012).
[9]C. Altintas, G. Avci, H. Daglar, E. Gulcay-Ozcan, I. Erucar, and S. Keskin, "Computer simulations of 4240 MOF membranes for H_2/CH_4 separations: Insights into structure–performance relations," J. Mater. Chem. A **6**(14), 5836–5847 (2018).
[10]G. Avci, I. Erucar, and S. Keskin, "Do new MOFs perform better for CO_2 capture and H_2 purification? Computational screening of the updated MOF database," ACS Appl. Mater. Interfaces **12**(37), 41567–41579 (2020).
[11]Q. Qian, P. A. Asinger, M. J. Lee, G. Han, K. Mizrahi Rodriguez, S. Lin, F. M. Benedetti, A. X. Wu, W. S. Chi, and Z. P. Smith, "MOF-based membranes for gas separations," Chem. Rev. **120**(16), 8161–8266 (2020).
[12]S. Budhathoki, O. Ajayi, J. A. Steckel, and C. E. Wilmer, "High-throughput computational prediction of the cost of carbon capture using mixed matrix membranes," Energy Environ. Sci. **12**(4), 1255–1264 (2019).
[13]S. Aydin, C. Altintas, I. Erucar, and S. Keskin, "Computational investigation of dual filler-incorporated polymer membranes for efficient CO_2 and H_2 separation: MOF/COF/polymer mixed matrix membranes," Ind. Eng. Chem. Res. **62**(6), 2924–2936 (2023).
[14]H. Demir, G. O. Aksu, H. C. Gulbalkan, and S. Keskin, "MOF membranes for CO_2 capture: Past, present and future," Carbon Capture Sci. Technol. **2**, 100026 (2022).
[15]H. Daglar and S. Keskin, "Recent advances, opportunities, and challenges in high-throughput computational screening of MOFs for gas separations," Coord. Chem. Rev. **422**, 213470 (2020).
[16]H. Demir and S. Keskin, "A new era of modeling MOF-based membranes: cooperation of theory and data science," Macromol. Mater. Eng. **309**(1), 2300225 (2024).
[17]P. Z. Moghadam, A. Li, S. B. Wiggin, A. Tao, A. G. Maloney, P. A. Wood, S. C. Ward, and D. Fairen-Jimenez, "Development of a Cambridge Structural Database subset: A collection of metal–organic frameworks for past, present, and future," Chem. Mater. **29**(7), 2618–2625 (2017).
[18]Y. G. Chung, E. Haldoupis, B. J. Bucior, M. Haranczyk, S. Lee, H. Zhang, K. D. Vogiatzis, M. Milisavljevic, S. Ling, and J. S. Camp, "Advances, updates, and analytics for the computation-ready, experimental metal–organic framework database: CoRE MOF 2019," J. Chem. Eng. Data **64**(12), 5985–5998 (2019).
[19]Y. G. Chung, J. Camp, M. Haranczyk, B. J. Sikora, W. Bury, V. Krungleviciute, T. Yildirim, O. K. Farha, D. S. Sholl, and R. Q. Snurr, "Computation-ready, experimental metal–organic frameworks: A tool to enable high-throughput screening of nanoporous crystals," Chem. Mater. **26**(21), 6185–6192 (2014).
[20]Y. G. Chung, E. Haldoupis, B. J. Bucior, M. Haranczyk, S. Lee, K. D. Vogiatzis, S. Ling, M. Milisavljevic, H. Zhang, J. S. Camp, B. Slater, J. Ilja Siepmann, D. S. Sholl, and R. Q. Snurr (2024), "Advances, updates, and analytics for the computation-ready, experimental metal–organic framework database: CoRE MOF 2019," Zenodo. https://doi.org/10.5281/zenodo.14184621
[21]M. Tong, Y. Lan, Z. Qin, and C. Zhong, "Computation-ready, experimental covalent organic framework for methane delivery: Screening and material design," J. Phys. Chem. C **122**(24), 13009–13016 (2018).
[22]D. Ongari, A. V. Yakutovich, L. Talirz, and B. Smit, "Building a consistent and reproducible database for adsorption evaluation in covalent–organic frameworks," ACS Cent. Sci. **5**(10), 1663–1675 (2019).
[23]M. S. Lohse and T. Bein, "Covalent organic frameworks: Structures, synthesis, and applications," Adv. Funct. Mater. **28**(33), 1705553 (2018).
[24]R. L. Martin and M. Haranczyk, "Construction and characterization of structure models of crystalline porous polymers," Cryst. Growth Des. **14**(5), 2431–2440 (2014).
[25]M. A. Addicoat, D. E. Coupry, and T. Heine, "AuToGraFS: Automatic topological generator for framework structures," J. Phys. Chem. A **118**(40), 9607–9614 (2014).
[26]Y. J. Colón, D. A. Gómez-Gualdrón, and R. Q. Snurr, "Topologically guided, automated construction of metal–organic frameworks and their evaluation for energy-related applications," Cryst. Growth Des. **17**(11), 5801–5810 (2017).
[27]X. Kong, H. Deng, F. Yan, J. Kim, J. A. Swisher, B. Smit, O. M. Yaghi, and J. A. Reimer, "Mapping of functional groups in metal-organic frameworks," Science **341**(6148), 882–885 (2013).
[28]C. E. Wilmer, M. Leaf, C. Y. Lee, O. K. Farha, B. G. Hauser, J. T. Hupp, and R. Q. Snurr, "Large-scale screening of hypothetical metal–organic frameworks," Nat. Chem. **4**(2), 83–89 (2012).
[29]S. Majumdar, S. M. Moosavi, K. M. Jablonka, D. Ongari, and B. Smit, "Diversifying databases of metal organic frameworks for high-throughput computational screening," ACS Appl. Mater. Interfaces **13**(51), 61004–61014 (2021).
[30]P. G. Boyd and T. K. Woo, "A generalized method for constructing hypothetical nanoporous materials of any net topology from graph theory," CrystEngComm **18**(21), 3777–3792 (2016).
[31]C. Gu, Z. Yu, J. Liu, and D. S. Sholl, "Construction of an anion-pillared MOF database and the screening of MOFs suitable for Xe/Kr separation," ACS Appl. Mater. Interfaces **13**(9), 11039–11049 (2021).
[32]Y. Lan, X. Han, M. Tong, H. Huang, Q. Yang, D. Liu, X. Zhao, and C. Zhong, "Materials genomics methods for high-throughput construction of COFs and targeted synthesis," Nat. Commun. **9**(1), 5274 (2018).
[33]J. S. De Vos, S. Borgmans, P. Van Der Voort, S. M. Rogge, and V. Van Speybroeck, "ReDD-COFFEE: A ready-to-use database of covalent organic framework structures and accurate force fields to enable high-throughput screenings," J. Mater. Chem. A **11**(14), 7468–7487 (2023).
[34]D. Dubbeldam, S. Calero, D. E. Ellis, and R. Q. Snurr, "RASPA: Molecular simulation software for adsorption and diffusion in flexible nanoporous materials," Mol. Simul. **42**(2), 81–101 (2016).
[35]A. P. Thompson, H. M. Aktulga, R. Berger, D. Bolintineanu, W. M. Brown, P. Crozier, P. J. in't Veld, A. Kohlmeyer, S. G. Moore, T. D. Nguyen, R. Shan, M. J. Stevens, J. Tranchida, C. Trott, and S. J. Plimpton, "LAMMPS - A flexible simulation tool for particle-based materials modeling at the atomic, meso, and continuum scales," Comput. Phys. Commun. **271**, 108171 (2022).
[36]X. Liu, J. Liu, S. Mao, H. Xu, Y. Wang, W. Tao, and Z. Li, "Molecular dynamics simulation of CO_2 permeation and separation in Zr-MOF membranes," Fluid Phase Equilib. **581**, 114073 (2024).
[37]R. C. Dutta and S. K. Bhatia, "Interfacial engineering of MOF-based mixed matrix membrane through atomistic simulations," J. Phys. Chem. C **124**(1), 594–604 (2020).
[38]S. Velioglu and S. Keskin, "Simulation of H_2/CH_4 mixture permeation through MOF membranes using non-equilibrium molecular dynamics," J. Mater. Chem. A **7**(5), 2301–2314 (2019).
[39]D. Frenkel and B. Smit, *Understanding Molecular Simulation: From Algorithms to Applications* (Elsevier, 2023).
[40]B. L. Eggimann, A. J. Sunnarborg, H. D. Stern, A. P. Bliss, and J. I. Siepmann, "An online parameter and property database for the TraPPE force field," Mol. Simul. **40**(1–3), 101–105 (2014).
[41]C. Murthy, K. Singer, M. Klein, and I. McDonald, "Pairwise additive effective potentials for nitrogen," Mol. Phys. **41**(6), 1387–1399 (1980).
[42]M. G. Martin and J. I. Siepmann, "Transferable potentials for phase equilibria. 1. United-atom description of *n*-alkanes," J. Phys. Chem. B **102**(14), 2569–2577 (1998).
[43]V. Buch, "Path integral simulations of mixed *para*-D_2 and *ortho*-D_2 clusters: The orientational effects," J. Chem. Phys. **100**(10), 7610–7629 (1994).
[44]J. Van Loef, "Transport properties of compressed atomic and molecular liquids, and solids and the molar volume," Physica B+ C **103**(2–3), 133–157 (1981).
[45]R.-M. Pellenq and P. Levitz, "Capillary condensation in a disordered mesoporous medium: A grand canonical Monte Carlo study," Mol. Phys. **100**(13), 2059–2077 (2002).
[46]A. K. Rappé, C. J. Casewit, K. Colwell, W. A. Goddard III, and W. M. Skiff, "UFF, a full periodic table force field for molecular mechanics and molecular dynamics simulations," J. Am. Chem. Soc. **114**(25), 10024–10035 (1992).
[47]S. L. Mayo, B. D. Olafson, and W. A. Goddard, "DREIDING: A generic force field for molecular simulations," J. Phys. Chem. **94**(26), 8897–8909 (1990).

14 October 2025 06:23:21

© Author(s) 2025

[48]M. Ernst, J. D. Evans, and G. Gryn'ova, "Host–guest interactions in framework materials: Insight from modeling," Chem. Phys. Rev. **4**(4), 041303 (2023).
[49]R. B. Getman, Y.-S. Bae, C. E. Wilmer, and R. Q. Snurr, "Review and analysis of molecular simulations of methane, hydrogen, and acetylene storage in metal–organic frameworks," Chem. Rev. **112**(2), 703–723 (2012).
[50]R. Mercado, B. Vlaisavljevich, L.-C. Lin, K. Lee, Y. Lee, J. A. Mason, D. J. Xiao, M. I. Gonzalez, M. T. Kapelewski, and J. B. Neaton, "Force field development from periodic density functional theory calculations for gas separation applications using metal–organic frameworks," J. Phys. Chem. C **120**(23), 12590–12604 (2016).
[51]M. Fischer, J. R. Gomes, M. Fröba, and M. Jorge, "Modeling adsorption in metal–organic frameworks with open metal sites: Propane/propylene separations," Langmuir **28**(22), 8537–8549 (2012).
[52]M. Fischer, B. Kuchta, L. Firlej, F. Hoffmann, and M. Fröba, "Accurate prediction of hydrogen adsorption in metal−organic frameworks with unsaturated metal sites via a combined density-functional theory and molecular mechanics approach," J. Phys. Chem. C **114**(44), 19116–19126 (2010).
[53]J. G. McDaniel, K. Yu, and J. Schmidt, "Ab initio, physically motivated force fields for CO_2 adsorption in zeolitic imidazolate frameworks," J. Phys. Chem. C **116**(2), 1892–1903 (2012).
[54]J. Fu and H. Sun, "An ab initio force field for predicting hydrogen storage in IRMOF materials," J. Phys. Chem. C **113**(52), 21815–21824 (2009).
[55]M. Tafipolsky, S. Amirjalayer, and R. Schmid, "First-principles-derived force field for copper paddle-wheel-based metal−organic frameworks," J. Phys. Chem. C **114**(34), 14402–14409 (2010).
[56]D. Yu, P. Ghosh, and R. Q. Snurr, "Hierarchical modeling of ammonia adsorption in functionalized metal–organic frameworks," Dalton Trans. **41**(14), 3962–3973 (2012).
[57]W. Li, S. Grimme, H. Krieg, J. Möllmann, and J. Zhang, "Accurate computation of gas uptake in microporous organic molecular crystals," J. Phys. Chem. C **116**(16), 8865–8871 (2012).
[58]A. Einstein, "On the theory of the Brownian movement," Ann. Phys. **19**(4), 371–381 (1906).
[59]H. Daglar, I. Erucar, and S. Keskin, "Recent advances in simulating gas permeation through MOF membranes," Mater. Adv. **2**(16), 5300–5317 (2021).
[60]D. Frenkel and B. Smit, *Understanding Molecular Simulation*, 2nd ed. (Academic Press, San Diego, CA, 2002).
[61]L. M. Robeson, "Correlation of separation factor versus permeability for polymeric membranes," J. Membr. Sci. **62**(2), 165–185 (1991).
[62]L. M. Robeson, "The upper bound revisited," J. Membr. Sci. **320**(1–2), 390–400 (2008).
[63]R. Pal, "Permeation models for mixed matrix membranes," J. Colloid Interface Sci. **317**(1), 191–198 (2008).
[64]J. C. Maxwell, *A Treatise on Electricity and Magnetism* (Clarendon Press, 1873).
[65]V. D. Bruggeman, "Berechnung verschiedener physikalischer Konstanten von heterogenen Substanzen. I. Dielektrizitätskonstanten und Leitfähigkeiten der Mischkörper aus isotropen Substanzen," Ann. Phys. **416**(7), 636–664 (1935).
[66]T. Lewis and L. Nielsen, "Dynamic mechanical properties of particulate-filled composites," J. Appl. Polym. Sci. **14**(6), 1449–1471 (1970).
[67]R. Pal, "New models for thermal conductivity of particulate composites," J. Reinf. Plast. Compos. **26**(7), 643–651 (2007).
[68]J. Felske, "Effective thermal conductivity of composite spheres in a continuous medium with contact resistance," Int. J. Heat Mass Transfer **47**(14–16), 3453–3461 (2004).
[69]R. Bouma, A. Checchetti, G. Chidichimo, and E. Drioli, "Permeation through a heterogeneous membrane: The effect of the dispersed phase," J. Membr. Sci. **128**(2), 141–149 (1997).
[70]I. Erucar and S. Keskin, "Computational methods for MOF/polymer membranes," Chem. Rec. **16**(2), 703–718 (2016).
[71]H. Yin, M. Xu, Z. Luo, X. Bi, J. Li, S. Zhang, and X. Wang, "Machine learning for membrane design and discovery," Green Energy Environ. **9**(1), 54–70 (2024).
[72]C. Altintas, O. F. Altundal, S. Keskin, and R. Yildirim, "Machine learning meets with metal organic frameworks for gas storage and separation," J. Chem. Inf. Model. **61**(5), 2131–2146 (2021).
[73]S. Chong, S. Lee, B. Kim, and J. Kim, "Applications of machine learning in metal-organic frameworks," Coord. Chem. Rev. **423**, 213487 (2020).
[74]T. F. Willems, C. H. Rycroft, M. Kazi, J. C. Meza, and M. Haranczyk, "Algorithms and tools for high-throughput geometry-based analysis of crystalline porous materials," Microporous Mesoporous Mater. **149**(1), 134–141 (2012).
[75]R. S. Olson, R. J. Urbanowicz, P. C. Andrews, N. A. Lavender, L. C. Kidd, and J. H. Moore, "Automating biomedical data science through tree-based pipeline optimization," in *19th European Conference on Applications of Evolutionary Computation (EvoApplications 2016)*, Porto, Portugal, March 30–April 1 (Springer, 2016), Part I 19, pp. 123–137.
[76]Q. Yao, M. Wang, Y. Chen, W. Dai, Y.-F. Li, W.-W. Tu, Q. Yang, and Y. Yu, "Taking human out of learning applications: A survey on automated machine learning," arXiv:1810.13306 (2018).
[77]P.-G. Martinsson, V. Rokhlin, and M. Tygert, "A randomized algorithm for the decomposition of matrices," Appl. Comput. Harmon. Anal. **30**(1), 47–68 (2011).
[78]L. Breiman, "Random forests," Mach. Learn. **45**, 5–32 (2001).
[79]G. James, D. Witten, T. Hastie, and R. Tibshirani, *An Introduction to Statistical Learning* (Springer, 2013).
[80]V. Vovk, "Kernel ridge regression," in *Empirical Inference: Festschrift in Honor of Vladimir N. Vapnik* (Springer, 2013), pp. 105–116.
[81]W. S. Noble, "What is a support vector machine?" Nat. Biotechnol. **24**(12), 1565–1567 (2006).
[82]M. Awad and R. Khanna, *Efficient Learning Machines: Theories, Concepts, and Applications for Engineers and System Designers* (Springer Nature, 2015).
[83]J. H. Friedman, "Stochastic gradient boosting," Comput. Stat. Data Anal. **38**(4), 367–378 (2002).
[84]A. K. Jain, J. Mao, and K. M. Mohiuddin, "Artificial neural networks: A tutorial," Computer **29**(3), 31–44 (1996).
[85]S. M. Lundberg, G. Erion, H. Chen, A. DeGrave, J. M. Prutkin, B. Nair, R. Katz, J. Himmelfarb, N. Bansal, and S.-I. Lee, "From local explanations to global understanding with explainable AI for trees," Nat. Mach. Intell. **2**(1), 56–67 (2020).
[86]H. Daglar and S. Keskin, "Combining machine learning and molecular simulations to unlock gas separation potentials of MOF membranes and MOF/polymer MMMs," ACS Appl. Mater. Interfaces **14**(28), 32134–32148 (2022).
[87]S. Zhang, Y. He, Z. Zhang, and C. Zhong, "Machine learning aided investigation on the structure-performance correlation of MOF for membrane-based He/H_2 separation," Green Chem. Eng. **5**(4), 526–532 (2024).
[88]X. Bai, Z. Shi, H. Xia, S. Li, Z. Liu, H. Liang, Z. Liu, B. Wang, and Z. Qiao, "Machine-learning-assisted high-throughput computational screening of metal–organic framework membranes for hydrogen separation," Chem. Eng. J. **446**, 136783 (2022).
[89]Q. Huang, X. Yuan, L. Li, Y. Yan, X. Yang, W. Wang, Y. Chen, H. Liang, H. Gao, and Y. Wu, "Machine learning and molecular fingerprint screening of high-performance 2D/3D MOF membranes for Kr/Xe separation," Chem. Eng. Sci. **280**, 119031 (2023).
[90]I. B. Orhan, H. Daglar, S. Keskin, T. C. Le, and R. Babarao, "Prediction of O_2/N_2 selectivity in metal–organic frameworks via high-throughput computational screening and machine learning," ACS Appl. Mater. Interfaces **14**(1), 736–749 (2022).
[91]H. Li, C. Wang, Y. Zeng, D. Li, Y. Yan, X. Zhu, and Z. Qiao, "Combining computational screening and machine learning to predict metal–organic framework adsorbents and membranes for removing CH_4 or H_2 from air," Membranes **12**(9), 830 (2022).
[92]Y. Situ, X. Yuan, X. Bai, S. Li, H. Liang, X. Zhu, B. Wang, and Z. Qiao, "Large-scale screening and machine learning for metal–organic framework membranes to capture CO_2 from flue gas," Membranes **12**(7), 700 (2022).
[93]Y. Yang, Z. Yu, and D. S. Sholl, "Machine learning models for predicting molecular diffusion in metal–organic frameworks accounting for the impact of framework flexibility," Chem. Mater. **35**(23), 10156–10168 (2023).
[94]M. Zhou, A. Vassallo, and J. Wu, "Toward the inverse design of MOF membranes for efficient D_2/H_2 separation by combination of physics-based and data-driven modeling," J. Membr. Sci. **598**, 117675 (2020).
[95]B. Xin, M. Feng, M. Cheng, Z. Dai, S. Ye, L. Zhou, Y. Dai, and X. Ji, "Combining interpretable machine learning and molecular simulation to

14 October 2025 06:23:21

© Author(s) 2025

advance the discovery of COF-based membranes for acid gas separation," Ind. Eng. Chem. Res. **63**(18), 8369–8382 (2024).
[96]J. Wu, Y. Guo, G. Liu, G. Liu, and W. Jin, "Machine learning accelerates high throughput design and screening of MOF mixed-matrix membranes towards He separation," J. Membr. Sci. **717**, 123612 (2025).
[97]J. Guan, T. Huang, W. Liu, F. Feng, S. Japip, J. Li, J. Wu, X. Wang, and S. Zhang, "Design and prediction of metal organic framework-based mixed matrix membranes for CO_2 capture via machine learning," Cell Rep. Phys. Sci. **3**(5), 100864 (2022).
[98]H. Wan, Y. Fang, M. Hu, S. Guo, Z. Sui, X. Huang, Z. Liu, Y. Zhao, H. Liang, and Y. Wu, "Interpretable machine-learning and big data mining to predict the CO_2 separation in polymer-MOF mixed matrix membranes," Adv. Sci. **12**(16), 2405905 (2025).
[99]L. Yao, Z. Zhang, Y. Li, J. Zhuo, Z. Chen, Z. Lin, H. Liu, and Z. Yao, "Precise prediction of CO_2 separation performance of metal–organic framework mixed matrix membranes based on feature selection and machine learning," Sep. Purif. Technol. **349**, 127894 (2024).
[100]Z. Zhang, X. Cao, C. Geng, Y. Sun, Y. He, Z. Qiao, and C. Zhong, "Machine learning aided high-throughput prediction of ionic liquid@ MOF composites for membrane-based CO_2 capture," J. Membr. Sci. **650**, 120399 (2022).
[101]Y. He, S. Zhang, and C. Zhong, "Unlocking the potential of ionic liquids in Anion-Pillared MOFs for enhanced He/H_2 separation Performance: A combined computational screening and Machine learning study," Sep. Purif. Technol. **363**, 132253 (2025).
[102]M. Alizamir, A. Keshavarz, F. Abdollahi, A. Khosravi, and S. Karagöz, "Accurately predicting the performance of MOF-based mixed matrix membranes for CO_2 removal using a novel optimized extreme learning machine by BAT algorithm," Sep. Purif. Technol. **325**, 124689 (2023).
[103]N. Habib, H. C. Gulbalkan, A. S. Aydogdu, A. Uzun, and S. Keskin, "Towards rational design of ionic liquid/metal-organic framework composites for efficient gas separations: Combining molecular modeling, machine learning, and experiments to move beyond trial-and-error," Coord. Chem. Rev. **539**, 216707 (2025).
[104]J. Usman, S. I. Abba, N. Baig, N. Abu-Zahra, S. W. Hasan, and I. H. Aljundi, "Design and machine learning prediction of in situ grown PDA-stabilized MOF (UiO-66-NH_2) membrane for low-pressure separation of emulsified oily wastewater," ACS Appl. Mater. Interfaces **16**(13), 16271–16289 (2024).
[105]Z. Cao, O. Barati Farimani, J. Ock, and A. Barati Farimani, "Machine learning in membrane design: From property prediction to AI-guided optimization," Nano Lett. **24**(10), 2953–2960 (2024).
[106]S. M. Moosavi, A. Chidambaram, L. Talirz, M. Haranczyk, K. C. Stylianou, and B. Smit, "Capturing chemical intuition in synthesis of metal-organic frameworks," Nat. Commun. **10**(1), 539 (2019).
[107]L. Pilz, C. Natzeck, J. Wohlgemuth, N. Scheuermann, S. Spiegel, S. Oßwald, A. Knebel, S. Bräse, C. Wöll, and M. Tsotsalas, "Utilizing machine learning to optimize metal–organic framework-derived polymer membranes for gas separation," J. Mater. Chem. A **11**(45), 24724–24737 (2023).
[108]D.-H. Chen, H. Gliemann, and C. Wöll, "Layer-by-layer assembly of metal-organic framework thin films: Fabrication and advanced applications," Chem. Phys. Rev. **4**(1), 011305 (2023).
[109]G. Tom, S. P. Schmid, S. G. Baird, Y. Cao, K. Darvish, H. Hao, S. Lo, S. Pablo-García, E. M. Rajaonson, and M. Skreta, "Self-driving laboratories for chemistry and materials science," Chem. Rev. **124**(16), 9633–9732 (2024).

14 October 2025 06:23:21

© Author(s) 2025